JAMES | Journal of Advances in Modeling Earth Systems

RESEARCH ARTICLE
10.1029/2022MS003532

Volcanic Drivers of Stratospheric Sulfur in GFDL ESM4

Chloe Yuchao Gao[1,2], Vaishali Naik[3], Larry W. Horowitz[3], Paul Ginoux[3], Fabien Paulot[3], John Dunne[3], Michael Mills[4], Valentina Aquila[5], and Peter Colarco[6]

[1]Program in Atmospheric and Oceanic Sciences, Princeton University, Princeton, NJ, USA, [2]Now at Department of Atmospheric and Oceanic Sciences, Institute of Atmospheric Sciences, Fudan University, Shanghai, China, [3]Geophysical Fluid Dynamics Laboratory, National Oceanic and Atmospheric Administration, Princeton, NJ, USA, [4]Atmospheric Chemistry Observations and Modeling Laboratory, National Center for Atmospheric Research, Boulder, CO, USA, [5]Department of Environmental Science, American University, Washington, DC, USA, [6]Atmospheric Chemistry and Dynamics Laboratory, NASA Goddard Space Flight Center, Greenbelt, MD, USA

Key Points:

- We present an interactive representation of the stratospheric sulfur cycle in GFDL ESM4 that replaced prescribed aerosol optical properties
- We simulated years 1989–2014 with a focus on the Mt. Pinatubo eruption and evaluated against observations
- Simulated stratospheric sulfate burden and optical depth are sensitive to injection height, emission amount, and aerosol size

Correspondence to:
C. Y. Gao,
chloe.gao@princeton.edu

Citation:
Gao, C. Y., Naik, V., Horowitz, L. W., Ginoux, P., Paulot, F., Dunne, J., et al. (2023). Volcanic drivers of stratospheric sulfur in GFDL ESM4. *Journal of Advances in Modeling Earth Systems*, *15*, e2022MS003532. https://doi.org/10.1029/2022MS003532

Received 23 NOV 2022
Accepted 1 MAY 2023

Abstract Stratospheric injections of sulfur dioxide from major volcanic eruptions perturb the Earth's global radiative balance and dominate variability in stratospheric sulfur loading. The atmospheric component of the GFDL Earth System Model (ESM4.1) uses a bulk aerosol scheme and previously prescribed the distribution of aerosol optical properties in the stratosphere. To quantify volcanic contributions to the stratospheric sulfur cycle and the resulting climate impact, we modified ESM4.1 to simulate stratospheric sulfate aerosols prognostically. Driven by explicit volcanic emissions of aerosol precursors and non-volcanic sources, we conduct ESM4.1 simulations from 1989 to 2014, with a focus on the Mt. Pinatubo eruption. We evaluate our interactive representation of the stratospheric sulfur cycle against data from Moderate Resolution Imaging Spectroradiometer, Multi-angle Imaging SpectroRadiometer, Advanced Very High Resolution Radiometer, High Resolution Infrared Radiation Sounder, and Stratospheric Aerosol and Gas Experiment II. To assess the key processes associated with volcanic aerosols, we performed a sensitivity analysis of sulfate burden from the Mt. Pinatubo eruption by varying injection heights, emission amount, and stratospheric sulfate's dry effective radius. We find that the simulated stratospheric sulfate mass burden and aerosol optical depth in the model are sensitive to these parameters, especially volcanic SO_2 injection height, and the optimal combination of parameters depends on the metric we evaluate.

Plain Language Summary Major volcanic eruptions emit sulfur dioxide into the stratosphere and affect the Earth's global radiative balance as well as the stratospheric sulfur abundance. The GFDL Earth System Model (ESM4.1) previously uses prescribed aerosol optical properties, and in this paper, we replace it with explicit volcanic emissions to study the volcanic contribution to the stratospheric sulfur cycle and its impact. We simulate years from 1989 to 2014, with a focus on the Mt. Pinatubo eruption as a benchmark. We also evaluate the new improvements against observations and performed sensitivity analyses of the sulfate burden from the Mt. Pinatubo eruptions. We find that the simulated stratospheric sulfate amount and aerosol optical depth are sensitive to injection height, emission amount, and aerosol size, and while the injection height is the most sensitive, the best combination of parameters depends on the chosen observational metric.

1. Introduction

Sulfur plays an important role in the stratosphere through chemical and radiative processes. Specifically, sulfate aerosols provide surfaces for ozone-depleting heterogeneous chemistry, absorb and scatter shortwave radiation, and absorb longwave radiation (Andronova et al., 1999; Ramachandran et al., 2000; Robock, 2000; Stenchikov et al., 1998; Stratospheric Processes and their Role in Climate [SPARC], 2010). The major source and driver of variability in the stratospheric sulfur budget are volcanic eruptions, which inject sulfur dioxide and sulfate aerosols into the stratosphere (Kremser et al., 2016). Once emitted, volcanic sulfur dioxide rapidly converts into gas-phase sulfuric acid or sulfate aerosols in the troposphere, but the process takes a few weeks in the stratosphere (Bluth et al., 1992).

The potential climate effect of sulfate aerosol from volcanic eruptions is more limited in the troposphere compared to the stratosphere due to the efficient wet removal by tropospheric clouds and dry deposition at the surface. On the other hand, powerful explosive volcanic eruptions that reach the lower stratosphere have led to perturbations to the Earth's global radiative balance that are detectable in observational temperature records, cooling the surface and

troposphere (Canty et al., 2013; McCormick et al., 1995; Minnis et al., 1993; Robock, 2000; Santer et al., 2014; Soden, 2002). The greater climate impact of stratospheric eruptions is mainly from the longer aerosol lifetime in the stratosphere, which allows volcanic aerosols to be distributed globally (Cole-Dai, 2010). Large volcanic eruptions are often considered a natural analog for sulfate aerosol geoengineering (or solar radiation management, or solar radiation modification, or stratospheric aerosol injection), the proposal to deliberately inject aerosol in the stratosphere to increase the albedo of the Earth and counter part of the warming associated with increasing greenhouse gas concentrations. In terms of sulfate forcing efficiency (sulfate forcing per unit of SO_2 emitted), eruptive volcanic sulfate is 5 times greater than anthropogenic sulfate (Ge et al., 2016). Additionally, stratospheric chemistry's response to major volcanic eruptions such as Mt. Pinatubo highlights the impact of volcanic eruptions on stratospheric ozone, whose mixing ratio decreases in the lower stratosphere and increases in the middle stratosphere, causing a net reduction in ozone under conditions with increased chlorine loading (Austin et al., 2013).

While the impact of major volcanic eruptions on the stratosphere has garnered increasing interest in recent years, modeling efforts to fully account for the chemistry and climate effects of direct volcanic sulfur injections into the stratosphere remain limited. In most Earth system models, the chemistry and climate effects of volcanic sulfate aerosols are typically represented by prescribing aerosol properties, such as stratospheric aerosol optical depth (AOD) and Surface Area Density (SAD), based on satellite observations (Zanchettin et al., 2016). A few studies have implemented the capability to simulate volcanic aerosol properties driven by volcanic emissions in their models (English et al., 2013; Ivy et al., 2017; Mills et al., 2016; Solomon et al., 2016; Timmreck, Graf, & Feichter, 1999, Timmreck, Graf, & Kirchner, 1999); these studies have improved the treatment of volcanic properties to realistically capture the distribution and effects of stratospheric sulfate aerosols.

The 1991 Mt. Pinatubo eruption is the largest eruption of the satellite record (1980-present), and observations from the event provided unprecedented data to aid modeling efforts, albeit precise quantification of the magnitude and altitude of the volcanic injection remains uncertain (Guo et al., 2004; Thomason, 1992). Past modeling studies of the Mt. Pinatubo eruption adopted different SO_2 emission mass and injection heights within the ranges identified by observations (Aquila et al., 2012, 2013; Brühl et al., 2014; Dhomse et al., 2014; English et al., 2013; Mills et al., 2016; Niemeier et al., 2009; Oman et al., 2006; Pitari & Mancini, 2002; Sheng et al., 2015a, 2015b; Toohey et al., 2011; Timmreck, Graf, & Feichter, 1999, Timmreck, Graf, & Kirchner, 1999; Zhao et al., 1995). Dhomse et al. (2014) and Sheng et al. (2015b) found the best agreement with Stratospheric Aerosol and Gas Experiment (SAGE) II observations when they prescribed an SO_2 injection between 10 and 14 Tg of SO_2. Mills et al. (2016) found that a 10 Tg SO_2 emissions in the Community Earth System Model/Whole Atmosphere Community Climate Model simulations produce a good agreement with the Total Ozone Mapping Spectrometer (TOMS, Bluth et al., 1992) and Television Infrared Observation Satellite Operational Vertical Sounder observations of volcanic SO_2 mass approximately a week after the eruption, which is when 99% of ice particles and ash, the portion that the authors considered "climatically relevant" were removed (Guo et al., 2004). They justified using an SO_2 injection that is lower than the observed by noting that models do not consider in-plume processes such as SO_2 scavenging by ash and ice particles, which are present in nature. Mills et al. (2016) also found that when emitting 12 Tg SO_2, their simulated AOD was overestimated compared to lidar observations. On the higher end of the range, Aquila et al. (2012) chose 20 Tg of SO_2 based on TOMS and found that emitting 5 Tg of SO_2 does not provide enough positive radiative feedback to sustain the lofting of the volcanic aerosol.

Similarly, past studies assumed widely varying SO_2 injection heights. Lidar observations detected aerosol layers at 19–23 km (Winker & Osborn, 1992), and Antuña et al. (2002) found the SO_2 injection height range to be 18–25 km. Aquila et al. (2012) performed an ensemble of experiments, with an initial injection height of 16–18 km and found that their model responded quickly to radiatively interacting aerosols, lofting the volcanic aerosol; whereas, Timmreck, Graf, and Feichter (1999) and Zhao et al. (1995) based their injection height on SAGE II observations at higher altitudes. The interactive stratospheric aerosol model intercomparison project by Timmreck et al. (2018, Table 9) and Quaglia et al. (2023; Figure 1) summarized the wide range of SO_2 emissions used in past modeling studies, with emissions ranging from 5 to 20 Tg and injection height ranging from 15 to 30 km. Lastly, for models that do not interactively simulate aerosol distribution, sulfate dry effective radius used for gravitational settling and optical properties is also varied in past literature, ranging from 0.166 to 1 μm (Aquila et al., 2012; Lacis, 2015; Li & Min, 2002; Li et al., 2001)). For models that simulate aerosol distribution, the effective radius varies depending on location, and they are calculated from Mie theory by integrating the scattering and extinction coefficients or using Mie-theory-based lookup tables (Quaglia et al., 2023).

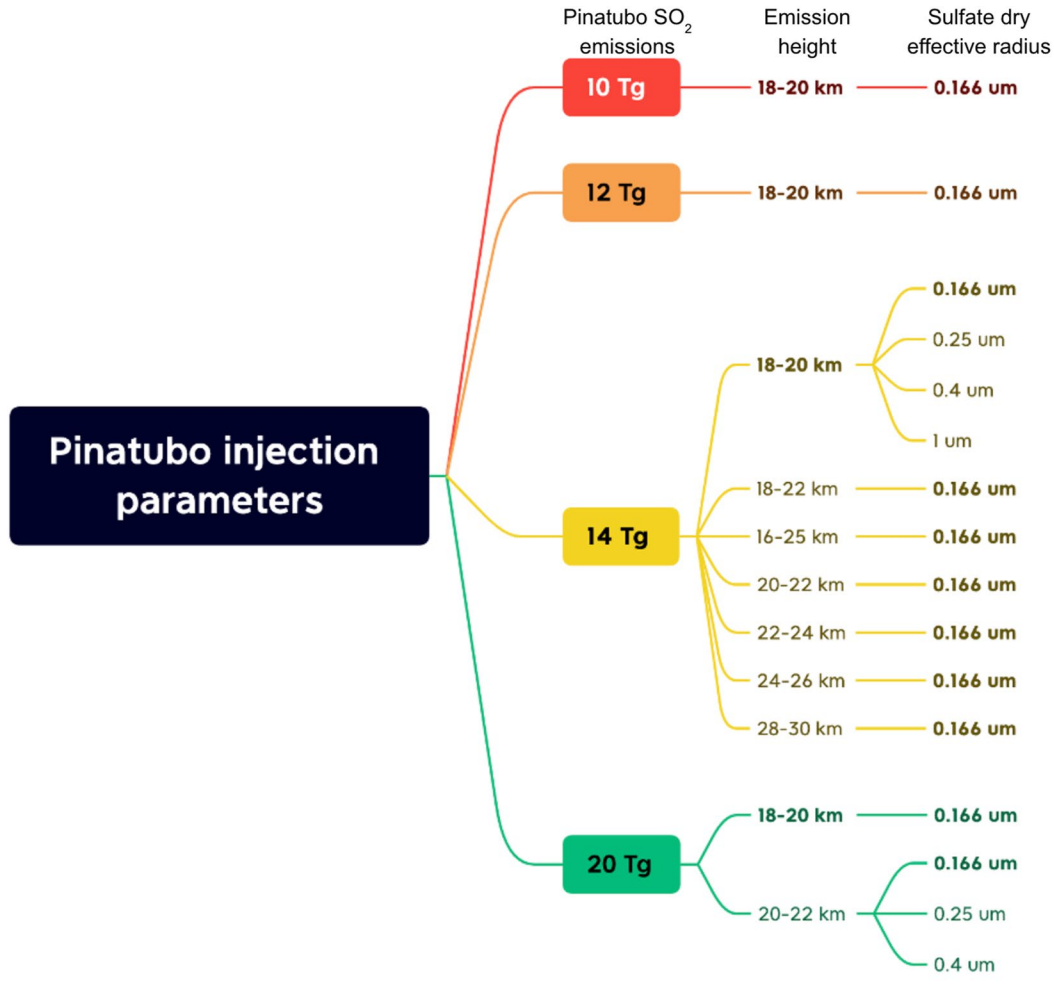

Figure 1. SO_2 emissions, injection height, and sulfate dry effective radius parameters used in sensitivity simulations.

Such a wide range of parameters used to model the same eruption is an indication that models are sensitive to the input for volcanic emissions. By testing our model's sensitivity to volcanic SO_2 injection amount, height, and particle size, we could gain insights into the critical processes associated with volcanic aerosols. Sulfate aerosol microphysics (i.e., formation and growth), co-emission with other species such as ash (Zhu et al., 2020), which are currently absent in most models; as well as aerosols' interaction with radiation and atmospheric dynamic biases in circulation (e.g., vertical lofting and transport).

In this study, we describe the improvements implemented in the Atmospheric Model (AM4.1) of the GFDL Earth System Model (ESM4.1) to replace the previously prescribed distributions of aerosol optical properties with the new capability to simulate stratospheric sulfur aerosols prognostically, driven by volcanic as well as non-volcanic sources. We show that an interactive representation of the stratospheric sulfur cycle in global climate models, driven by explicit volcanic emissions of aerosol precursors and coupled with the chemistry and radiation schemes, could capture the multiple interactions between the sulfur cycle and climate change and variability. We used this newly developed model capability to simulate the 1989 to 2014 period, focusing on the 1991 Mt. Pinatubo volcanic eruption as a perturbation and benchmark event for model evaluation. We share insights learned from this experiment and discuss comparisons of our results against observations as well as the control ESM4.1 version with prescribed volcanic aerosol forcing.

2. Model Description

In this study we use GFDL Earth System Model version 4.1 (ESM4.1; Dunne et al., 2020) and focus on updating its atmospheric component, AM4.1 (Horowitz et al., 2020). AM4.1 is a standalone atmospheric physics and chemistry model for atmospheric applications and includes interactive tropospheric and stratospheric gas-phase and aerosol chemistry. Its mass-based aerosol scheme transports 18 prognostic aerosol tracers, including bulk sulfate aerosols (SO_4^{2-}). The combined tropospheric and stratospheric chemistry scheme includes 58 prognostic gas-phase tracers, five prognostic ideal tracers, and 40 non-transported diagnostic chemical tracers, with 43 photolysis reactions, 190 gas-phase kinetic reactions, and 15 heterogeneous reactions. In the standard AM4.1 configuration, sulfur is assumed to be in aerosol form, and gas-phase H_2SO_4 is not explicitly represented. Sulfur tracers included in the chemical mechanism are sulfur dioxide (SO_2), sulfate aerosol, and dimethyl sulfide. The heterogeneous oxidation of SO_2 to sulfate on pre-existing sulfate and nitrate aerosols, following Zheng et al. (2015), is also included.

2.1. Model Updates

We build on the bulk aerosol approach used in AM4.1, in which total sulfate mass is a prognostic variable, to calculate the stratospheric aerosol distribution interactively and prognostically. Following Mills et al. (2016, 2017), we implemented volcanic SO_2 emissions from the VolcanEESM (Volcanic Emissions for Earth System Models) database compiled by Neely and Schmidt (2016). This database includes SO_2 emissions from volcanic eruptions injected into both the troposphere and stratosphere. Total volcanic SO_2 emissions are uniformly distributed vertically between the minimum and maximum altitudes of the eruption plume and emitted in the model grid box containing the latitude and longitude of the volcano. Similarly to Mills et al. (2016, 2017), volcanic SO_2 is emitted at a constant emission rate over a 6-hr period between 12:00 UTC and 18:00 UTC on the day of the eruption. We also scale the heterogeneous uptake of SO_2 by NO_2 to avoid destabilization in the simulation run.

The calculation of volcanic aerosol SAD for stratospheric heterogeneous reaction rates is also updated. Instead of calculating SAD from aerosol extinction centered at 1.0 μm using a simple parameterization (Thomason et al., 1997), we used the emission-driven sulfate concentrations, with an assumed effective radius of 0.166 μm. To account for both volcanic and non-volcanic sources of stratospheric sulfate aerosols, we also added carbonyl sulfide (OCS) to the existing chemical mechanism, including its oxidation and photolysis to SO_2 in the stratosphere.

Lower boundary conditions for OCS were specified based on data from Montzka et al. (2004). For stratospheric sulfate aerosol removal, we implemented the sedimentation of sulfate aerosols in the stratosphere, based on the existing dust and sea salt aerosol sedimentation scheme, and assign a sulfate dry effective radius for the calculation. We note here that sectional or modal microphysics approach might produce different results, which would affect sedimentation (i.e., Dhomse et al., 2021; Visioni et al., 2022), and that these results also depend on altitude or location.

2.2. Simulations

We assess the skill of our updated model, including volcanic emissions and sedimentation, by comparing a 1984–2014 simulation carried out using prescribed volcanic aerosol optical properties (PRESC simulation), analog to the previous version of the model, to a simulation that exercises the new capabilities (VOLC simulation), that is, with explicit volcanic emissions (replacing the prescribed volcanic optical properties) and sulfate sedimentation. The simulations are driven by observed sea-surface temperature and sea-ice from reconstruction, and horizontal winds are nudged to NCEP-NCAR reanalysis to facilitate consistent comparisons with observations (Kalnay et al., 1996). These simulations are used to test the influence of model updates on stratospheric sulfur distribution and AOD. Non-volcanic emissions of aerosols and aerosol precursors, as well as the parameterizations used for non-volcanic aerosol, are identical in the PRESC and VOLC simulations.

Given the large range used in the literature for SO_2 emissions and injection height from the Mt. Pinatubo eruption, we performed sensitivity tests to evaluate the model sensitivity to these inputs. Our default VOLC simulation emits 14 Tg volcanic SO_2 at a height of 18–20 km. Considering measurement-based emission amounts as well as candidates used in previous studies (Section 1), we chose 10, 12, 14, and 20 Tg of SO_2 mass emissions and injection heights at 16–25, 18–22, 20–22, and 28–30 km (Figure 1).

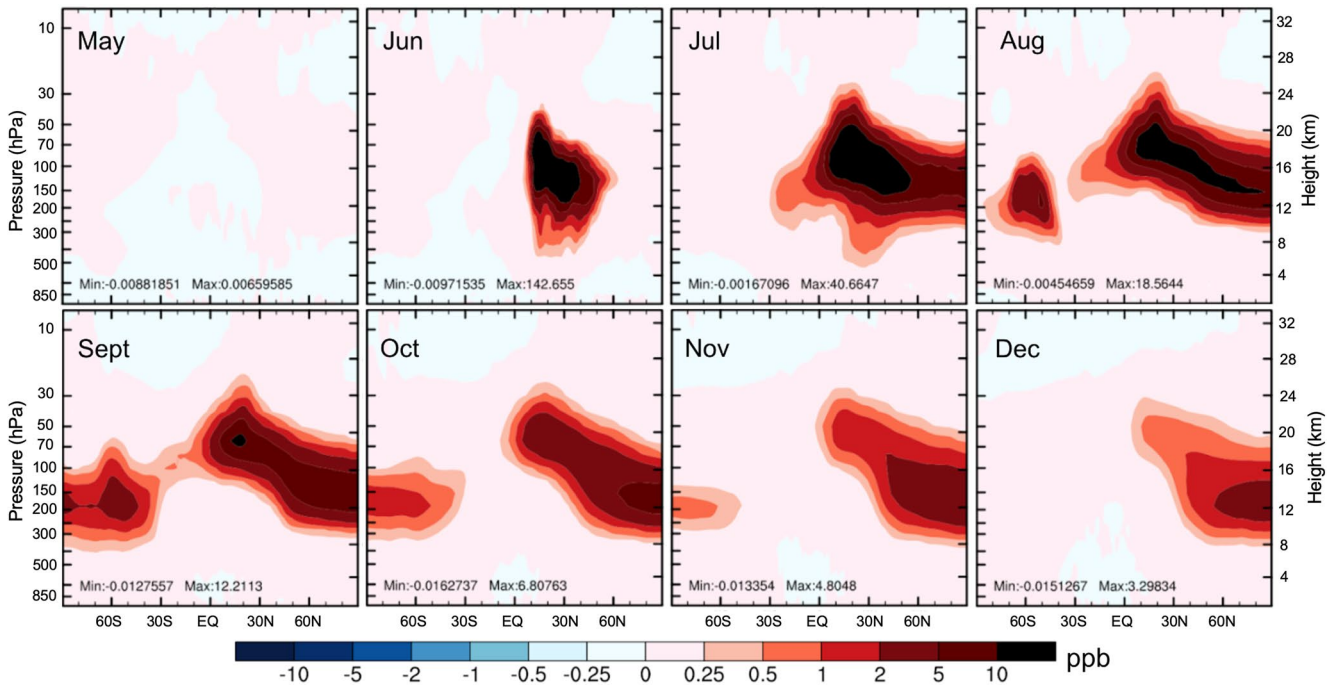

Figure 2. Differences in simulated monthly average zonal mean SO_2 (in ppbv) between the two simulations (VOLC-PRESC) from May to December 1991.

The dry effective radius used in the settling parameterization determines the sulfate settling velocity and, consequently, the simulated sulfate burden and distribution. Since in our mass-based aerosol scheme the settling effective radius is chosen independently from the radius used in the calculation of the aerosol optical properties, we also performed a suite of sensitivity tests varying the dry sulfate effective radius. Based on the aerosol radii used in previous studies (Aquila et al., 2012; Lacis, 2015; Li & Min, 2002; Li et al., 2001), the radii we tested are 0.25 μm, which Lacis (2015) used as the effective radius size for mature volcanic aerosols; 0.4 μm, which Aquila et al. (2012) calculated based on a lognormally distributed aerosol with a median radius of 0.35 μm and a standard deviation of 1.25; 1 μm, which is assumed to be the largest volcanic aerosol size; and 0.166 μm, the settling radius used in our default simulation, which is calculated assuming a lognormal distribution with a median radius of 0.05 μm and a standard deviation of 2, as used by Li et al. (2001) and Li and Min (2002). All simulation parameters and experiments are listed in Figure 1 (default simulation parameters are in bold).

3. Results

3.1. Comparison With Observations

We use the Mt. Pinatubo eruption as a benchmark event and focus on the months before and after the eruption. Figure 2 shows the difference in the monthly average zonal mean SO_2 mixing ratio from May to December in 1991. Since the PRESC simulation does not include SO_2 from volcanic sources but does account for that from OCS, the VOLC-PRESC difference shown in Figure 2 represents the SO_2 from Mt. Pinatubo and Cerro Hudson only. In June 1991, when Mt. Pinatubo erupted, the zonal SO_2 difference in Figure 2 shows the concentrated initial SO_2 injection in the VOLC simulation, which created a hotspot. The SO_2 plume evolves and spreads meridionally due to transport and stratospheric chemistry over the next few months.

As the SO_2 difference decreases with time, we find sulfate rapidly formed after the SO_2 mass dispersed. In June, when the eruption occurred, there is only a weak sulfate difference between VOLC and PRESC because of a delay in its formation from the injected SO_2 (Figure 3). In the following months, volcanic SO_4 increases while SO_2 is converted into SO_4. The e-folding time of the volcanic SO_2 decay corresponds to approximately a month, which is consistent with previous modeling studies. SO_4 is formed rapidly from SO_2 oxidation as shown in Figure 3, and its concentration increases with an e-folding time of approximately 1 month, similar to other modeling studies (Aquila et al., 2012).

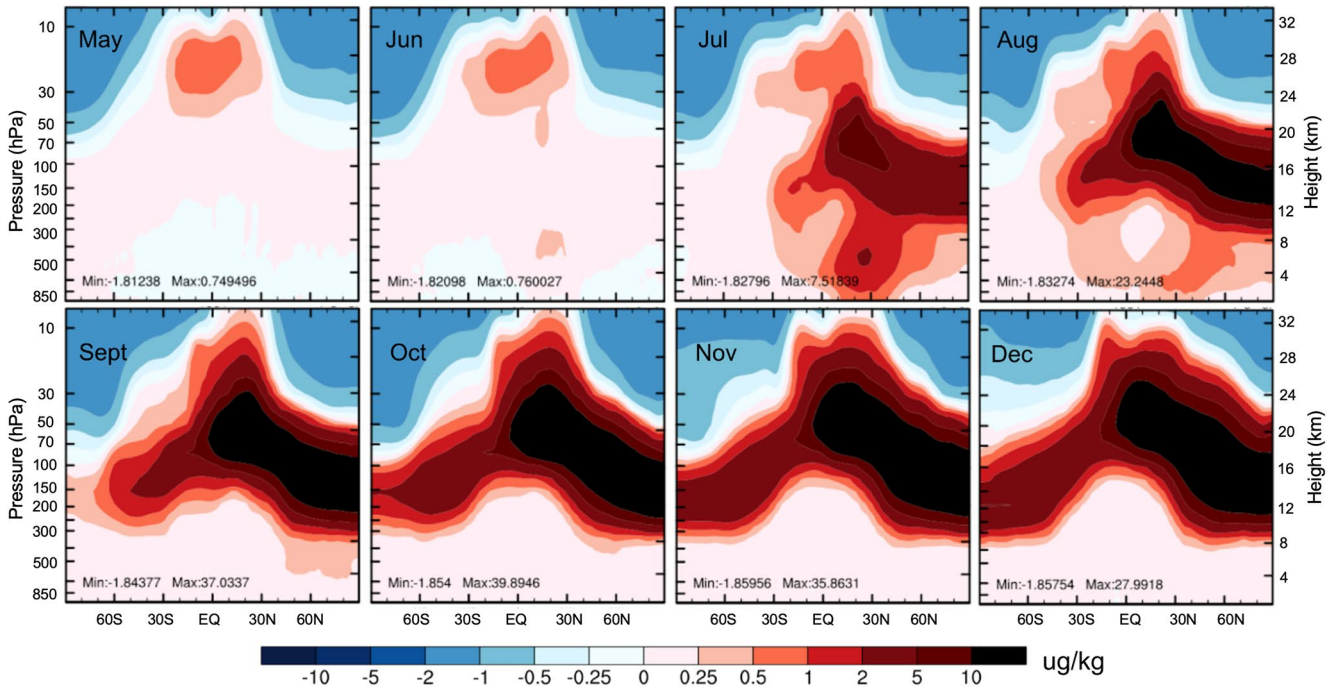

Figure 3. Differences in simulated monthly average zonal mean SO_4 mass mixing ratio (μg/kg) between the two simulations (VOLC-PRESC) from May to December 1991.

We also examined the total AOD following the Mt. Pinatubo eruption. Figure 4 shows the spatial AOD difference between the VOLC and PRESC experiments. The VOLC-PRESC difference in AOD follows the increase in SO_4 concentration with time, and it becomes widespread starting from July 1991. As time evolves, the volcanic aerosol spreads latitudinally, shifting more toward the Northern Hemisphere, which is consistent with the zonal sulfate concentration (Figure 3) and is likely due to circulation.

We also evaluated the AOD from 1999 to 2014 against observations from the Multi-angle Imaging SpectroRadiometer (MISR, Kahn et al., 2009) and Moderate Resolution Imaging Spectroradiometer (Levy et al., 2013) satellite instruments. The time evolution of AOD in VOLC and PRESC simulations overlap and compare similarly (except during the Mt. Pinatubo eruption). They also compare well against observations in recent years, despite being generally lower than observed (Figure 5).

As mentioned previously, enhanced volcanic aerosols perturb stratospheric chemistry and result in a net decrease in the ozone column. Therefore, we evaluated ozone from both the VOLC and the PRESC simulations against Solar Backscatter Ultra-Violet multi-satellite merged ozone total column (Frith, 2013) and the National Institute

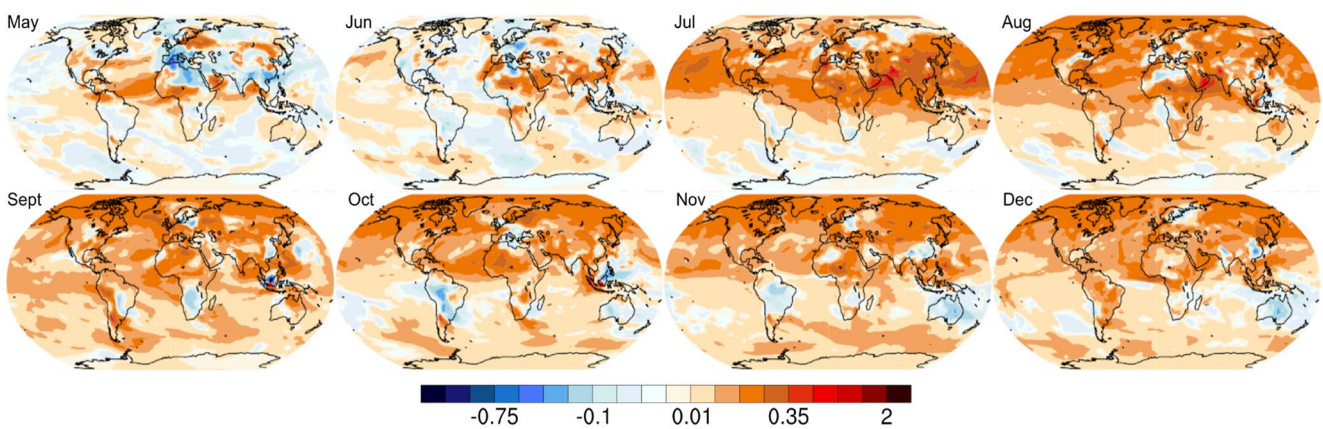

Figure 4. Differences in simulated monthly average total aerosol optical depth between VOLC and PRESC (VOLC-PRESC) for May–December 1991.

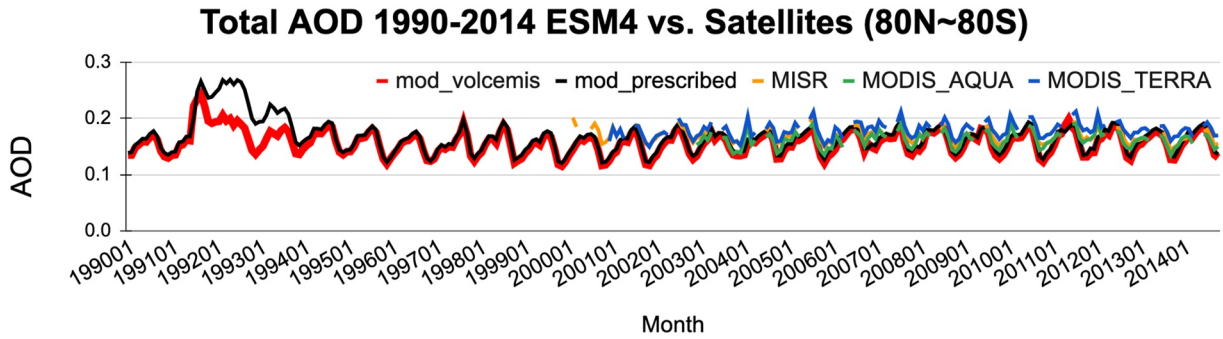

Figure 5. Timeseries of total global mean aerosol optical depth for VOLC and PRESC simulations compared against Moderate Resolution Imaging Spectroradiometer and Multi-angle Imaging SpectroRadiometer satellite retrievals.

of Water and Atmospheric Research-Bodeker Scientific total column ozone database (Bodeker et al., 2005). Both simulations reproduce the observed total ozone column well, with the PRESC simulation having a slightly low bias in the tropics and the VOLC simulation with a high bias in the northern midlatitudes, and PRESC has a more evident ozone depletion post-eruption than VOLC does (Figure 6). Overall, the two schemes show similar skills in simulating total column ozone trends.

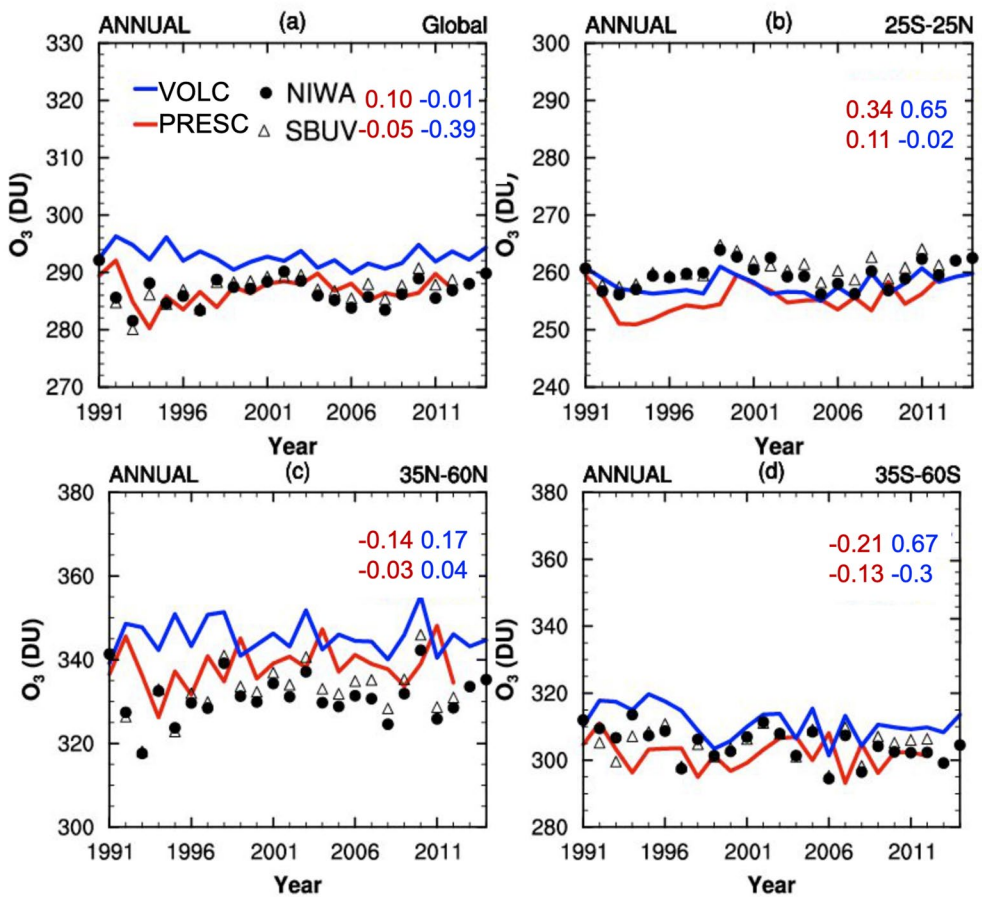

Figure 6. Comparison of timeseries of total ozone column for the annual mean (a) 90°S–90°N, (b) 25°S–25°N, (c) 35°N–60°N, (d) 35°S–60°S from the PRESC simulation (red) and the VOLC simulation (blue) against multi-satellite merged ozone total column (SBUV, Frith, 2013) in open triangles and the NIWA-BS total column ozone database (Bodeker et al., 2005) in closed circles. Correlation coefficients are listed at the top row for NIWA and the bottom row for SBUV.

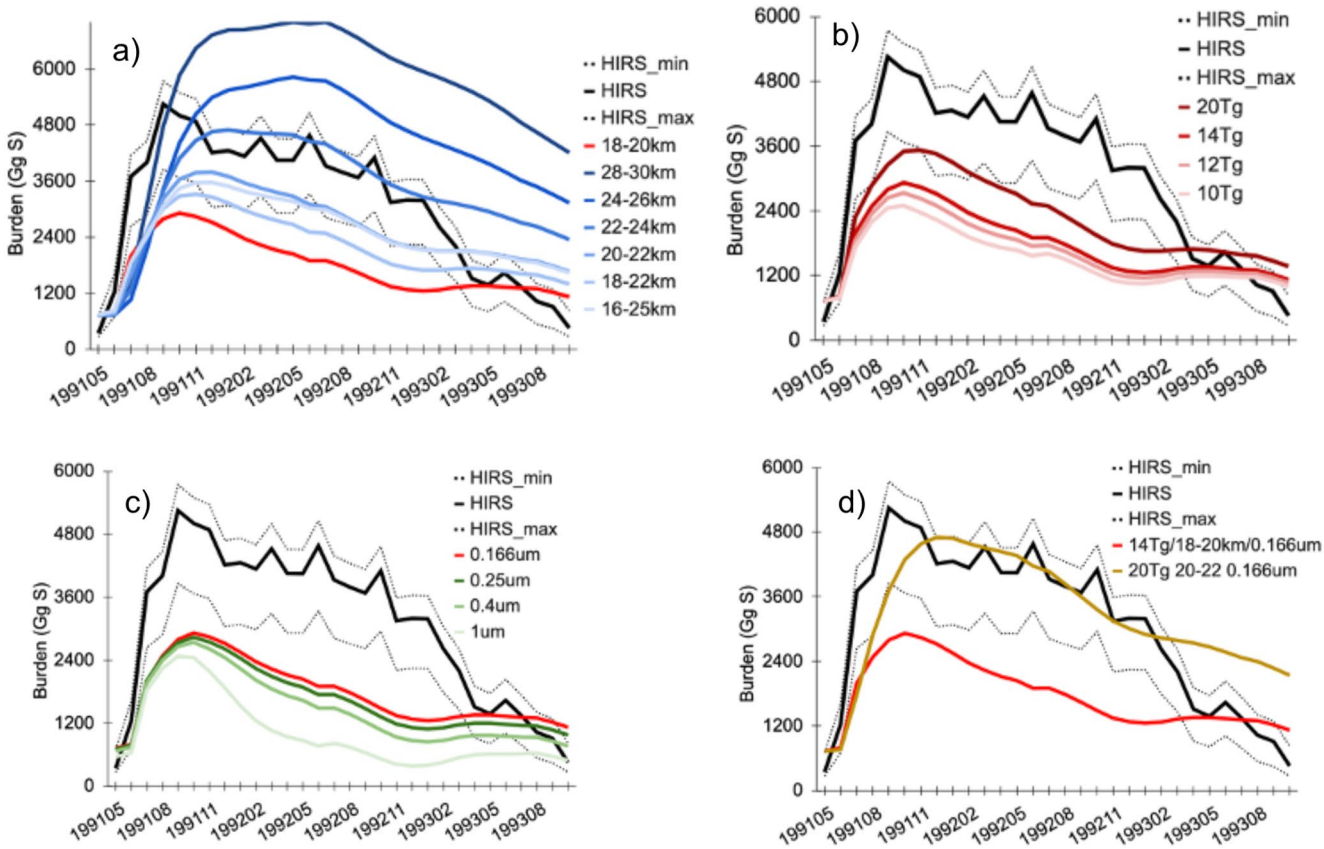

Figure 7. Timeseries of the global mass burden of sulfate for sensitivity runs compared against High Resolution Infrared Radiation Sounder with (a) varying injection height, (b) varying SO_2 emission amount, (c) varying sulfate dry effective radius, and (d) combination of parameters. The default VOLC simulation is in red.

3.2. Model Sensitivity to Injection Parameters

We evaluated the results from the sensitivity tests listed in Figure 1 against the High Resolution Infrared Radiation Sounder (HIRS) observations (Baran & Foot, 1994) (Figure 7). Each sub-plot in Figure 7 shows a group of simulations that have varying injection heights (Figure 7a), SO_2 emission amount (Figure 7b), or sulfate dry effective radius (Figure 7c). The default VOLC simulation, evaluated in the previous section, is in red as a reference.

We find that higher injection heights result in a larger sulfate mass burden and a longer atmospheric residence time of the sulfate particles, due to slower sedimentation from higher altitudes and slower transport to the troposphere by the Brewer-Dobson circulation. Next, we explore the sensitivity of sulfate mass burden to the injected SO_2 emission amount. As expected, since SO_2 is a source for sulfate formation, their magnitudes are directly proportional, we find that the greater emission amount leads to a higher burden, especially in the initial months. Then we checked the sensitivity of sulfate mass burden to sulfate dry effective radius, which is used in the gravitational settling calculations for sulfate sedimentation. We find that the sulfate burden in simulations with bigger sulfate particles declines faster, corresponding to shorter lifetimes. This is because sulfate dry effective radius directly affects sedimentation efficiency, with larger particles removed faster, leading to a steeper decline for the sulfate mass burden.

Our simulations show that sulfate mass burden is qualitatively most sensitive to changes in injection height, then emission amount, followed by sulfate dry effective radius, although the three parameters have different units and are not quantitatively comparable. It is likely that the sensitivity to injection height is also affected by the dynamics and radiation parameterizations used in the model. Overall, the simulation that results in the best agreement with HIRS observations is the one simulating the Mt. Pinatubo eruption with a 20 Tg SO_2 injection at 20–22 km

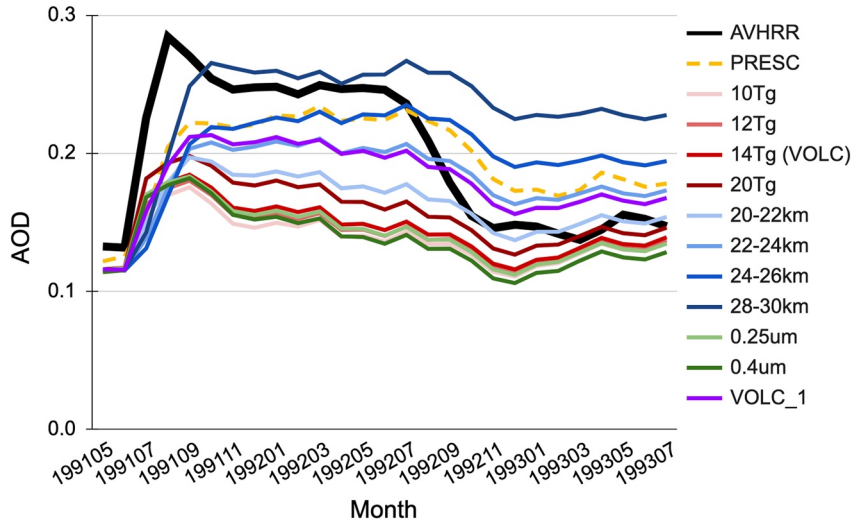

Figure 8. Timeseries of total aerosol optical depth over oceans for PRESC and VOLC sensitivity runs compared against Advanced Very High Resolution Radiometer from 1991 to 1993. The default VOLC simulation is indicated by the red line, and the VOLC_1 simulation is indicated by the purple line.

with the default sulfate dry effective radius of 0.166 μm. These parameters fall within the value range used in previous studies; this scenario will be referred to as VOLC_1 hereafter.

Using AOD as a metric, we also find varying parameters affect AOD. As mentioned previously, AOD from both VOLC and PRESC simulations compare well against recent satellite data, but observing capabilities were limited at the time of the eruption. In Figure 8, we show a comparison against Advanced Very High Resolution Radiometer (AVHRR) data over the oceans, where the observations were performed. Our PRESC and VOLC simulations do not capture well the peak AOD observed by AVHRR. Sensitivity tests with varying SO_2 emission amounts, SO_2 injection heights, and sulfate dry effective radii show that AOD is sensitive to all three parameters as well. Similar to sulfate mass burden, total AOD is most sensitive to SO_2 injection height. Results also suggest that a combination of parameter changes is needed to match AVHRR.

It is also worth noting that the best-case scenario VOLC_1 from the sulfate mass burden sensitivity simulations is not necessarily the best-matched one when using AOD as the metric, and when compared against AVHRR, the sulfate mass burden from every scenario seems to lack representation. Also, although it seems arbitrary to just test different heights and amounts, it guides our understanding of the sensitivity of burden and AOD to these parameters and the climate response, which would be very important when we investigate the impact of climate intervention. For example, for geoengineering purposes, we predict that it would be critical to quantify the short- and long-term effects on climate of injecting a specific amount at a certain height.

Lastly, we examined the radiative impacts of our changes in the representation of stratospheric sulfate by comparing the net radiative fluxes at the top of the atmosphere from the PRESC and VOLC_1 simulations (Figure 9). We find that the two simulations perform similarly, both capturing the decrease in net flux in the months following the Mt. Pinatubo eruption. We also compared the top of the atmosphere near-global (60°S–60°N) radiation anomalies against the Earth Radiation Budget Satellite (ERBS) observations (Allan et al., 2014; Liu et al., 2015). Figure 10 shows the monthly mean model output and the 72-day mean ERBS observations, both deseasonalized, plotted as anomalies from the 1985–1989 base period. The two simulations show similar anomaly trends, indicating that the interactive representation of volcanic stratospheric sulfate aerosol performs similarly to prescribed aerosols for the volcanic radiative forcing in our model.

4. Conclusion

Here we present an updated version of the atmospheric component AM4.1 of the GFDL ESM4.1, in which we replace the prescribed distribution of aerosol optical properties with a newly implemented prognostic simulation

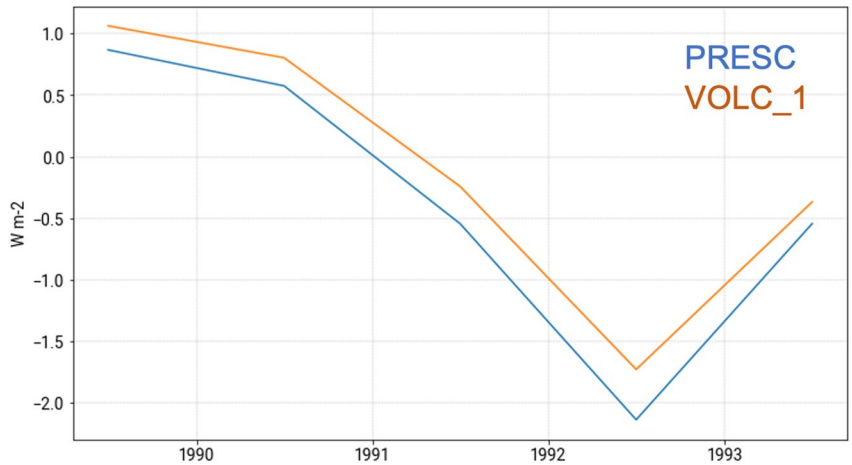

Figure 9. Top of the atmosphere all-sky global net radiation fluxes (W/m^2) for PRESC and VOLC_1 simulations from 1989 to 1994.

of stratospheric sulfur aerosols, driven by volcanic and non-volcanic sources. Since the developments are more relevant for volcanically active years, we used the Mt. Pinatubo eruption as a benchmark to evaluate the simulated stratospheric aerosol distribution and properties and explore their sensitivity to uncertainties in emission amount, injection height, and particle size. We explore the sensitivity of sulfate mass burden and AOD to various parameters (injection amount and height of SO_2 as well as dry effective radius of sulfate), in recognition of the importance of this sensitivity for understanding the response and impact of climate intervention. We find that, for our model, stratospheric sulfate mass burden and AOD are most sensitive to volcanic SO_2 injection height. We identify combinations of SO_2 injection height and amount that best match observations, although the optimal parameters vary based on the observational metric used.

Accurately simulating volcanic eruptions and their climate effects requires further improvements of our model, and several challenges remain for future studies. First, there are few measurements available for evaluation of our simulation of the Mt. Pinatubo eruption. Second, missing aerosol size evolution in our model likely led to inaccurate sedimentation, given that in the current version, sulfate dry effective radius is only used in the sedimentation calculation and remains constant. With a dynamic size distribution, we would be able to track the growth of particles, allowing for quicker settling of bigger particles in the initial months after a major volcanic eruption. Third, qualitative comparisons against other modeling studies show that different dynamics and physics parameterizations could lead to varying results using the same set of parameters described here, and a thorough modeling study would be needed to investigate the impact that different dynamics schemes have on stratospheric volcanic aerosols.

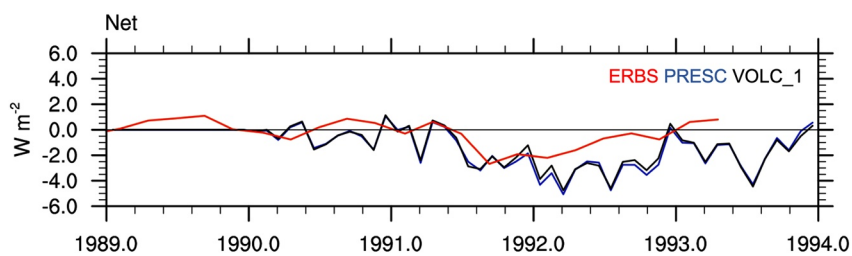

Figure 10. Top of the atmosphere near global (60°S–60°N) radiation anomalies (W/m^2) for PRESC (blue) and VOLC_1(black) simulations from 1989 to 1994 (vs. 1985–1989 base period) compared against ERBS (red).

Data Availability Statement

The model code is provided online at http://doi.org/10.5281/zenodo.3836405 (Dunne et al., 2020a). The input data used in the simulations are provided at GFDL's Data Portal ftp://data1.gfdl.noaa.gov/users/ESM4/ESM4Documentation/GFDL-ESM4/inputData/ESM4_rundir.tar.gz (Dunne et al., 2020b). The simulation output is provided online at https://doi.org/10.5281/zenodo.7799138 (Gao, 2023). MODIS data are available at http://dx.doi.org/10.5067/MODIS/MOD04_L2.006 ((Terra and Aqua, Levy et al., 2015)), MISR data are available at https://doi.org/10.5067/Terra/MISR/MIL3YRD_L3.005 (NASA/LARC/SD/ASDC, 2008), and AVHRR data are available at https://doi.org/10.25921/w3zj-4y48 (Zhao & NOAA CDR Program et al., 2022).

Acknowledgments
This work and CYG are supported by the NOAA Climate Program Office Earth's Radiation Budget Grant. VA is supported by the NASA Interdisciplinary Science (IDS) program (Grant 80NSSC20K1773). PRC was supported by the Chemistry-Climate Modeling (CCM) work-package from NASA's Modeling, Analysis, and Prediction Program (Grant 600-17-6985). We appreciate the editors and three anonymous reviewers for their supportive and insightful input during the revision.

References

Allan, R. P., Liu, C., Loeb, N. G., Palmer, M. D., Roberts, M., Smith, D., & Vidale, P. L. (2014). Changes in global net radiative imbalance 1985–2012. *Geophysical Research Letters*, *41*(15), 5588–5597. https://doi.org/10.1002/2014GL060962

Andronova, N. G., Rozanov, E. V., Yang, F., Schlesinger, M. E., & Stenchikov, G. L. (1999). Radiative forcing by volcanic aerosols from 1850 to 1994. *Journal of Geophysical Research*, *104*(D14), 16807–16826. https://doi.org/10.1029/1999jd900165

Antuña, J. C., Robock, A., Stenchikov, G. L., Thomason, L. W., & Barnes, J. E. (2002). Lidar validation of SAGE II aerosol measurements after the 1991 Mount Pinatubo eruption. *Journal of Geophysical Research*, *107*(D14), ACL3-1–ACL3-11. https://doi.org/10.1029/2001jd001441

Aquila, V., Oman, L. D., Stolarski, R., Douglass, A. R., & Newman, P. A. (2013). The response of ozone and nitrogen dioxide to the eruption of Mt. Pinatubo at southern and northern midlatitudes. *Journal of the Atmospheric Sciences*, *70*(3), 894–900. https://doi.org/10.1175/jas-d-12-0143.1

Aquila, V., Oman, L. D., Stolarski, R. S., Colarco, P. R., & Newman, P. A. (2012). Dispersion of the volcanic sulfate cloud from a Mount Pinatubo–like eruption. *Journal of Geophysical Research*, *117*(D6), 1984–2012. https://doi.org/10.1029/2011jd016968

Austin, J., Horowitz, L. W., Schwarzkopf, M. D., Wilson, R. J., & Levy, H., II. (2013). Stratospheric ozone and temperature simulated from the preindustrial era to the present day. *Journal of Climate*, *26*(11), 3528–3543. https://doi.org/10.1175/jcli-d-12-00162.1

Baran, A. J., & Foot, J. S. (1994). New application of the operational sounder HIRS in determining a climatology of sulphuric acid aerosol from the Pinatubo eruption. *Journal of Geophysical Research: Atmospheres (1984–2012)*, *99*(D12), 25673–25679. https://doi.org/10.1029/94jd02044

Bluth, G. J. S., Doiron, S. D., Schnetzler, C. C., Krueger, A. J., & Walter, L. S. (1992). Global tracking of the SO_2 clouds from the June, 1991 Mount Pinatubo eruptions. *Geophysical Research Letters*, *19*(2), 151–154. https://doi.org/10.1029/91gl02792

Bodeker, G. E., Shiona, H., & Eskes, H. (2005). Indicators of Antarctic ozone depletion. *Atmospheric Chemistry and Physics*, *5*(10), 2603–2615. https://doi.org/10.5194/acp-5-2603-2005

Brühl, C., Lelieveld, J., Tost, H., Höpfner, M., & Glatthor, N. (2014). Stratospheric sulfur and its implications for radiative forcing simulated by the chemistry climate model EMAC. *Journal of Geophysical Research: Atmospheres*, *120*(5), 2103–2118. https://doi.org/10.1002/2014jd022430

Canty, T., Mascioli, N. R., Smarte, M. D., & Salawitch, R. J. (2013). An empirical model of global climate—Part 1: A critical evaluation of volcanic cooling. *Atmospheric Chemistry and Physics*, *13*(8), 3997–4031. https://doi.org/10.5194/acp-13-3997-2013

Cole-Dai, J. (2010). Volcanoes and climate. *Wiley Interdisciplinary Reviews: Climate Change*, *1*(6), 824–839. https://doi.org/10.1002/wcc.76

Dhomse, S. S., Arosio, C., Feng, W., Rozanov, A., Weber, M., & Chipperfield, M. P. (2021). ML-TOMCAT: Machine-learning-based satellite-corrected global stratospheric ozone profile data set from a chemical transport model. *Earth System Science Data*, *13*(12), 5711–5729. https://doi.org/10.5194/essd-13-5711-2021

Dhomse, S. S., Emmerson, K. M., Mann, G. W., Bellouin, N., Carslaw, K. S., Chipperfield, M. P., et al. (2014). Aerosol microphysics simulations of the Mt.~Pinatubo eruption with the UM-UKCA composition-climate model. *Atmospheric Chemistry and Physics*, *14*(20), 11221–11246. https://doi.org/10.5194/acp-14-11221-2014

Dunne, J. P., Horowitz, L. W., Adcroft, A., Ginoux, P., Held, I. M., John, J., et al. (2020b). NOAA-GFDL/ESM4: GFDL Earth system model 4 (version ESM4). [Dataset]. ftp://data1.gfdl.noaa.gov/users/ESM4/ESM4Documentation/GFDL-ESM4/inputData/ESM4_rundir.tar.gz

Dunne, J. P., Horowitz, L. W., Adcroft, A., Ginoux, P., Held, I. M., John, J., et al. (2020a). NOAA-GFDL/ESM4: GFDL Earth system model 4 (version ESM4) [Model code]. *Zenodo*. https://doi.org/10.5281/zenodo.3836405

Dunne, J. P., Horowitz, L. W., Adcroft, A. J., Ginoux, P., Held, I. M., John, J. G., et al. (2020). The GFDL Earth system model version 4.1 (GFDL-ESM 4.1): Overall coupled model description and simulation characteristics. *Journal of Advances in Modeling Earth Systems*, *12*(11). https://doi.org/10.1029/2019ms002015

English, J. M., Toon, O. B., & Mills, M. J. (2013). Microphysical simulations of large volcanic eruptions: Pinatubo and Toba: Microphysics of Pinatubo/Toba eruptions. *Journal of Geophysical Research: Atmospheres*, *118*(4), 1880–1895. https://doi.org/10.1002/jgrd.50196

Frith, S. M. (2013). *Multi-satellite merged ozone (O3) profile and total column monthly L3 global 5.0deg Lat zones, version 1*. NASA Goddard Earth Science Data and Information Services Center (GES DISC).

Gao, C. Y. (2023). ESM4 stratospheric aerosol output [Dataset]. Zenodo. https://doi.org/10.5281/zenodo.7799138

Ge, C., Wang, J., Carn, S., Yang, K., Ginoux, P., & Krotkov, N. (2016). Satellite-based global volcanic SO_2 emissions and sulfate direct radiative forcing during 2005–2012. *Journal of Geophysical Research: Atmospheres*, *121*(7), 3446–3464. https://doi.org/10.1002/2015JD023134

Guo, S., Bluth, G. J. S., Rose, W. I., Watson, I. M., & Prata, A. J. (2004). Re-evaluation of SO_2 release of the 15 June 1991 Pinatubo eruption using ultraviolet and infrared satellite sensors. *Geochemistry, Geophysics, Geosystems*, *5*(4), Q04001. https://doi.org/10.1029/2003GC000654

Horowitz, L. W., Naik, V., Paulot, F., Ginoux, P. A., Dunne, J. P., Mao, J., et al. (2020). The GFDL global atmospheric chemistry-climate model AM4.1: Model description and simulation characteristics. *Journal of Advances in Modeling Earth Systems*, *12*(10). https://doi.org/10.1029/2019ms002032

Ivy, D. J., Solomon, S., Kinnison, D., Mills, M. J., Schmidt, A., & Neely, R. R. (2017). The influence of the Calbuco eruption on the 2015 Antarctic ozone hole in a fully coupled chemistry-climate model. *Geophysical Research Letters*, *44*(5), 2556–2561. https://doi.org/10.1002/2016gl071925

Kahn, R. A., Nelson, D. L., Garay, M. J., Levy, R. C., Bull, M. A., Diner, D. J., et al. (2009). MISR aerosol product attributes and statistical comparisons with MODIS. *IEEE Transactions on Geoscience and Remote Sensing*, *47*(12), 4095–4114. https://doi.org/10.1109/tgrs.2009.2023115

Kalnay, E., Kanamitsu, M., Kistler, R., Collins, W., Deaven, D., Gandin, L., et al. (1996). The NCEP/NCAR 40-year reanalysis project. *Bulletin of the American Meteorological Society*, *77*(3), 437–471. https://doi.org/10.1175/1520-0477(1996)077<0437:tnyrp>2.0.co;2

Kremser, S., Thomason, L. W., von Hobe, M., Hermann, M., Deshler, T., Timmreck, C., et al. (2016). Stratospheric aerosol—Observations, processes, and impact on climate. *Reviews of Geophysics*, *54*(2), 278–335. https://doi.org/10.1002/2015rg000511

Lacis, A. (2015). Volcanic aerosol radiative properties. *Past global change magazine* (Vol. 23, pp. 50–51). https://doi.org/10.22498/pages.23.2.50
Levy, R., Hsu, C., et al. (2015). MODIS atmosphere L2 aerosol product. NASA MODIS adaptive processing system [Dataset]. Goddard Space Flight Center. https://doi.org/10.5067/MODIS/MOD04_L2.006
Levy, R. C., Mattoo, S., Munchak, L. A., Remer, L. A., Sayer, A. M., Patadia, F., & Hsu, N. C. (2013). The collection 6 MODIS aerosol products over land and ocean. *Atmospheric Measurement Techniques*, *6*(11), 2989–3034. https://doi.org/10.5194/amt-6-2989-2013
Li, J., & Min, Q. (2002). Parameterization of the optical properties of sulfate aerosols in the infrared. *Journal of the Atmospheric Sciences*, *59*(21), 3130–3140. https://doi.org/10.1175/1520-0469(2002)059<3130:potopo>2.0.co;2
Li, J., Wong, J. G. D., Dobbie, J. S., & Chýlek, P. (2001). Parameterization of the optical properties of sulfate aerosols. *Journal of the Atmospheric Sciences*, *58*(2), 193–209. https://doi.org/10.1175/1520-0469(2001)058<0193:potopo>2.0.co;2
Liu, C., Allan, R. P., Berrisford, P., Mayer, M., Hyder, P., Loeb, N., et al. (2015). Combining satellite observations and reanalysis energy transports to estimate global net surface energy fluxes 1985–2012. *Journal of Geophysical Research: Atmospheres*, *120*, 9374–9389. https://doi.org/10.1002/2015JD023264
McCormick, M. P., Thomason, L. W., & Trepte, C. R. (1995). Atmospheric effects of the Mt Pinatubo eruption. *Nature*, *373*(6513), 399–404. https://doi.org/10.1038/373399a0
Mills, M. J., Richter, J. H., Tilmes, S., Kravitz, B., MacMartin, D. G., Glanville, A. A., et al. (2017). Radiative and chemical response to interactive stratospheric sulfate aerosols in fully coupled CESM1 (WACCM). *Journal of Geophysical Research: Atmospheres*, *122*(23), 13061–13078. https://doi.org/10.1002/2017jd027006
Mills, M. J., Schmidt, A., Easter, R., Solomon, S., Kinnison, D. E., Ghan, S. J., et al. (2016). Global volcanic aerosol properties derived from emissions, 1990-2014, using CESM1 (WACCM). *Journal of Geophysical Research: Atmospheres*, *121*(5), 2332–2348. https://doi.org/10.1002/2015jd024290
Minnis, P., Harrison, E. F., Stowe, L. L., Gibson, G. G., Denn, F. M., Doelling, D. R., & Smith, W. L. (1993). Radiative climate forcing by the Mount Pinatubo eruption. *Science*, *259*(5100), 1411–1415. https://doi.org/10.1126/science.259.5100.1411
Montzka, S. A., Aydin, M., Battle, M., Butler, J. H., Saltzman, E. S., Hall, B. D., et al. (2004). A 350-year atmospheric history for carbonyl sulfide inferred from Antarctic firn air and air trapped in ice. *Journal of Geophysical Research*, *109*, D22302. https://doi.org/10.1029/2004JD004686
NASA/LARC/SD/ASDC. (2008). MISR level 3 component global radiance product covering a year V005 [Dataset]. NASA Langley Atmospheric Science Data Center DAAC. https://doi.org/10.5067/Terra/MISR/MIL3YRD_L3.005
Neely, R. R. III., & Schmidt, A. (2016). VolcanEESM: Global volcanic sulphur dioxide (SO_2) emissions database from 1850 to present—Version 1.0. https://doi.org/10.5285/76ebdc0b-0eed-4f70-b89e-55e606bcd568
Niemeier, U., Timmreck, C., Graf, H.-F., Kinne, S., Rast, S., & Self, S. (2009). Initial fate offline ash and sulfur from large volcanic eruptions. *Atmospheric Chemistry and Physics*, *9*(22), 9043–9057. https://doi.org/10.5194/acp-9-9043-2009
Oman, L., Robock, A., Stenchikov, G. L., Thordarson, T., Koch, D., Shindell, D. T., & Gao, C. (2006). Modeling the distribution of the volcanic aerosol cloud from the 1783–1784 Laki eruption. *Journal of Geophysical Research*, *111*(D12), D12209. https://doi.org/10.1029/2005jd006899
Pitari, G., & Mancini, E. (2002). Short-term climatic impact of the 1991 volcanic eruption of Mt. Pinatubo and effects on atmospheric tracers. *Natural Hazards and Earth System Sciences*, *2*(1/2), 91–108. https://doi.org/10.5194/nhess-2-91-2002
Quaglia, I., Timmreck, C., Niemeier, U., Visioni, D., Pitari, G., Brodowsky, C., et al. (2023). Interactive stratospheric aerosol models' response to different amounts and altitudes of SO_2 injection during the 1991 Pinatubo eruption. *Atmospheric Chemistry and Physics*, *23*(2), 921–948. https://doi.org/10.5194/acp-23-921-2023
Ramachandran, S., Ramaswamy, V., Stenchikov, G. L., & Robock, A. (2000). Radiative impact of the Mount Pinatubo volcanic eruption: Lower stratospheric response. *Journal of Geophysical Research*, *105*(D19), 24409–24429. https://doi.org/10.1029/2000jd900355
Robock, A. (2000). Volcanic eruptions and climate. *Reviews of Geophysics*, *38*(2), 191–219. https://doi.org/10.1029/1998rg000054
Santer, B. D., Bonfils, C., Painter, J. F., Zelinka, M. D., Mears, C., Solomon, S., et al. (2014). Volcanic contribution to decadal changes in tropospheric temperature. *Nature Geoscience*, *7*(3), 185–189. https://doi.org/10.1038/ngeo2098
Sheng, J. X., Weisenstein, D. K., Luo, B. P., Rozanov, E., Arfeuille, F., & Peter, T. (2015a). A perturbed parameter model ensemble to investigate 1991 Mt Pinatubo's initial sulfur mass emission. *Atmospheric Chemistry and Physics Discussions*, *15*(4), 4601–4625. https://doi.org/10.5194/acpd-15-4601-2015
Sheng, J.-X., Weisenstein, D. K., Luo, B.-P., Rozanov, E., Stenke, A., Anet, J., et al. (2015b). Global atmospheric sulfur budget under volcanically quiescent conditions: Aerosol-chemistry-climate model predictions and validation. *Journal of Geophysical Research: Atmospheres*, *120*(1), 256–276. https://doi.org/10.1002/2014JD021985
Soden, B. J., Wetherald, R. T., Stenchikov, G. L., & Robock, A. (2002). Global cooling after the eruption of Mount Pinatubo: A test of climate feedback by water vapor. *Science*, *296*(5568), 727–730. https://doi.org/10.1126/science.296.5568.727
Solomon, S., Ivy, D. J., Kinnison, D., Mills, M. J., Neely, R. R., & Schmidt, A. (2016). Emergence of healing in the Antarctic ozone layer. *Science*, *353*(6296), 269–274. https://doi.org/10.1126/science.aae0061
Stenchikov, G. L., Kirchner, I., Robock, A., Graf, H., Antuña, J. C., Grainger, R. G., et al. (1998). Radiative forcing from the 1991 Mount Pinatubo volcanic eruption. *Journal of Geophysical Research*, *103*(D12), 13837–13857. https://doi.org/10.1029/98jd00693
Stratospheric Processes and their Role in Climate. (2010). In V. Eyring, T. G. Shepherd, & D. W. Waugh (Eds.), *SPARC CCMVal report on the evaluation of chemistry-climate models*. SPARC Rep. 5, WCRP-30/2010, WMO/TD - 40 Retrieved from www.sparc-climate.org/publications/sparc-reports/
Thomason, L. W. (1992). Observations of a new SAGE II aerosol extinction mode following the eruption of Mt. Pinatubo. *Geophysical Research Letters*, *19*(21), 2179–2182. https://doi.org/10.1029/92GL02185
Thomason, L. W., Poole, L. R., & Deshler, T. (1997). A global climatology of stratospheric aerosol surface area density deduced from stratospheric aerosol and gas experiment II measurements: 1984–1994. *Journal of Geophysical Research*, *102*(D7), 8967–8976. https://doi.org/10.1029/96JD02962
Timmreck, C., Graf, H.-F., & Feichter, J. (1999). Simulation of Mt. Pinatubo volcanic aerosol with the Hamburg climate model ECHAM4. *Theoretical and Applied Climatology*, *62*(3–4), 85–108. https://doi.org/10.1007/s007040050076
Timmreck, C., Graf, H.-F., & Kirchner, I. (1999b). A one and half year interactive MA/ECHAM4 simulation of Mount Pinatubo Aerosol. *Journal of Geophysical Research*, *104*(D8), 9337–9359. https://doi.org/10.1029/1999jd900088
Timmreck, C., Mann, G. W., Aquila, V., Hommel, R., Lee, L. A., Schmidt, A., et al. (2018). The interactive stratospheric aerosol model intercomparison project (ISA-MIP): Motivation and experimental design. *Geoscientific Model Development*, *11*(7), 2581–2608. https://doi.org/10.5194/gmd-11-2581-2018
Toohey, M., Krüger, K., Niemeier, U., & Timmreck, C. (2011). The influence of eruption season on the global aerosol evolution and radiative impact of tropical volcanic eruptions. *Atmospheric Chemistry and Physics*, *11*(23), 12351–12367. https://doi.org/10.5194/acp-11-12351-2011

Visioni, D., Tilmes, S., Bardeen, C., Mills, M., MacMartin, D. G., Kravitz, B., & Richter, J. H. (2022). Limitations of assuming internal mixing between different aerosol species: A case study with sulfate geoengineering simulations. *Atmospheric Chemistry and Physics*, *22*(3), 1739–1756. https://doi.org/10.5194/acp-22-1739-2022

Winker, D. M., & Osborn, M. T. (1992). Airborne lidar observations of the Pinatubo volcanic plume. *Geophysical Research Letters*, *19*(2), 167–170. https://doi.org/10.1029/91gl02867

Zanchettin, D., Khodri, M., Timmreck, C., Toohey, M., Schmidt, A., Gerber, E. P., et al. (2016). The model intercomparison project on the climatic response to Volcanic forcing (VolMIP): Experimental design and forcing input data for CMIP6. *Geoscientific Model Development*, *9*(8), 2701–2719. https://doi.org/10.5194/gmd-9-2701-2016

Zhao, J., Turco, R. P., & Toon, O. B. (1995). A model simulation of Pinatubo volcanic aerosols in the stratosphere. *Journal of Geophysical Research*, *100*(D4), 7315–7328. https://doi.org/10.1029/94jd03325

Zhao, X., & NOAA CDR Program. (2022). NOAA climate data record (CDR) of AVHRR daily and monthly aerosol optical thickness over global oceans, version 4.0 [Dataset]. NOAA National Centers for Environmental Information. https://doi.org/10.25921/w3zj-4y48

Zheng, B., Zhang, Q., Zhang, Y., He, K. B., Wang, K., Zheng, G. J., et al. (2015). Heterogeneous chemistry: A mechanism missing in current models to explain secondary inorganic aerosol formation during the January 2013 haze episode in North China. *Atmospheric Chemistry and Physics*, *15*(4), 2031–2049. https://doi.org/10.5194/acp-15-2031-2015

Zhu, Y., Toon, O. B., Jensen, E. J., Bardeen, C. G., Mills, M. J., Tolbert, M. A., et al. (2020). Persisting volcanic ash particles impact stratospheric SO_2 lifetime and aerosol optical properties. *Nature Communications*, *11*(1), 4526. https://doi.org/10.1038/s41467-020-18352-5